EFFECT OF WIND ON CRYOGENIC HYDROGEN DISPERSION FROM VENT STACKS

Ethan S. Hecht[a], and Nick J. Killingsworth[b]

[a]**Combustion Research Facility, Sandia National Laboratories, P.O. Box 969, MS 9052, Livermore, CA, 94551, USA, ehecht@sandia.gov**

[b]**Lawrence Livermore National Laboratory, 7000 East Ave., Livermore, CA, 94550, USA**

ABSTRACT

Liquid hydrogen vent stacks often release hydrogen, for example, due to pressure relief from an underutilized tank boiling off hydrogen or after hydrogen delivery and transfer (trucks often depressurize through the tank vent stack to meet pressure regulations for on-road transport). A rapid release of cryogenic hydrogen through a vent stack will condense moisture from the entrained air, forming a visible cloud. It is often assumed that the extent of the cold hydrogen is concurrent with the cloud. In this work, a laser-based Raman scattering diagnostic was used to map out the hydrogen location during a series of vent stack release experiments. A description of the diagnostic instrument is given, followed by a comparison of hydrogen signals to the visible cloud for releases through a liquid hydrogen vent stack. A liquid hydrogen pump was used to vary the flowrate of hydrogen through the vent stack and tests were performed under low and high wind conditions as well as low and high humidity conditions. The hydrogen was observed only where the condensed moisture was located, regardless of the humidity level or wind. These measurements are being used to validate models such as those included in Sanda's HyRAM toolkit and inform safety codes and standards.

1.0 INTRODUCTION

Liquid hydrogen is a promising medium to deliver and store large amounts of fuel for a variety of hydrogen energy applications. It is significantly denser than compressed gaseous hydrogen, unless under extreme pressure (190 MPa at ambient temperature). There are challenges with liquid hydrogen, some stemming from the fact that it is only a liquid at very low temperatures ($\approx$ 20 K at ambient pressure). This means that heat leak in even the most well insulated tanks will cause some of the liquid hydrogen to vaporize and build pressure. To prevent overpressurization of liquid hydrogen tanks (if underutilized), they are meant to safely vent hydrogen and are all equipped with vent stacks. Another significant challenge with liquid hydrogen in the United States is that the safety codes and standards that govern the siting of liquid hydrogen storage tanks, *NFPA 2 Hydrogen Technologies Code* [1] contains exposure distances from liquid hydrogen tanks that can be difficult to meet in constrained (e.g., urban) areas.

Several groups have performed experiments on cryogenic hydrogen in order to better understand its properties, validate models, and enable analyses that can provide justification for updates to fire codes. Xiao et al. [2] performed horizontal discharges of room temperature and cryogenic (80 K) hydrogen at pressures from 8.25–68.5 bar through 1 and 2 mm orifices, where concentration measurements were taken at several locations downstream of the release point. Friedrich et al. [3] also performed horizontal discharges of cryogenic (34–65 K) hydrogen at pressures up to 35 bar through 0.5 and 1 mm orifices, with measurements of flame properties as well as centerline concentration. Panda and Hecht [4] measured lab scale flames of hydrogen with release temperatures from 46–295 K, through nozzles from 0.75–1.25 mm, at pressures from 1–5 bar_g. Hecht

and Panda [5] performed lab-scale releases through 1 mm and 1.25 mm nozzles, from 2–5 bar of 45–82 K cryogenic hydrogen. Two-dimensional average mole fraction and temperature fields of these releases were measured using planar laser Raman imaging. Chowdhury and Hecht [6] measured cryogenic hydrogen dispersion under similar conditions as Hecht and Panda [5], but using rectangular, high aspect ratio nozzles, with the same cross-sectional area as a 1 mm diameter round orifice. Hecht and Chowdhury [7] measured cryogenic hydrogen flames for similar conditions as Panda and Hecht [4], but using rectangular, high aspect ratio nozzles, with the same cross-sectional area as a 1 mm diameter round orifice. The Pre-normative Research for Safe use of Liquid Hydrogen (PreSLHy) project funded by the European Fuel Cells and Hydrogen Joint Undertaking (FCH JU) studied several aspects of liquid hydrogen behavior. In one series of experiments, hydrogen at high pressures (5–200 bar) and ambient to low temperatures (80 K) was discharged through a series of orifices from 0.5–4 mm, measuring the conditions within the tank as well as the temperature and concentration at several locations outside the tank [8]. Common to all of these works is that the orifices are small (0.5–4 mm). While these small orifices are representative of leaks from a liquid hydrogen system, they are small relative to a vent stack release. These experiments are also designed to have little influence from the ambient environment (e.g., wind).

Larger releases while monitoring dispersion have been performed by several groups [9–15], but each of these experiments had rather sparse measurements of temperature and concentrations. In one case, there was no flammable mass observed outside the visible plume [9], but in another, the flammable mass extended well above the visible plume and was dependent on the ambient conditions [10]. Additional experiments under the PreSLHy program have been completed with finer resolution of concentration sensors [16], with ongoing analysis of the dispersion characteristics. Temporal variations in wind and other conditions during these larger experiments make data analysis and model validation challenging. There is still considerable uncertainty and a need for additional data on the large scale interactions of cryogenic hydrogen and the atmosphere. This work provides additional data and understanding on the behavior of cryogenic hydrogen and its dispersion in the atmosphere.

2.0 EXPERIMENTAL DESCRIPTION

Previously, it was shown that spontaneous Raman scattering from a high powered light source (i.e., laser) can be used to measure the concentration and temperature of cryogenic hydrogen dispersion [5, 6]. In this work, the same principles for the diagnostic were used but outside the laboratory. The third harmonic of a 10 Hz pulsed Nd-YAG laser (at 355 nm) with approximately 150 mJ/pulse was focused to a point approximately 9 m away from the laser (Spectra-Physics GCR-150). A high powered mirror in a 2D-motorized gimbal mount (Zaber T-OMG) enabled the laser to be rastered up to 7 degrees in both directions from the central alignment point. A diode within the laser housing captured a signal proportional to the shot-to-shot variability in power output of the laser. The laser was directed within 10 degrees of vertical, with beam blocks extending up to 7 ft (2.1 m) of height from the ground protecting workers against any misalignment or stray reflections. A gated ICCD camera (Princeton Instruments PIMAX II) with a 25mm focal length, f/0.95 lens (Angenieux) outfitted with two 10 nm half-width, 420 nm central wavelength, OD 4 band-pass filters was offset from the illumination to capture the spontaneous Raman scattering from hydrogen, which will be shifted from 355 nm to 416.5 nm. It should be noted that this signal is unique to scattering from hydrogen molecules. Aside from background light, there is no signal from other molecules within this wavelength range. In addition to the Raman camera, two visible cameras (Teledyne Dalsa Genie Nano-C2590) also captured images of the scene at the same frame-rate (10 Hz). One of the visible cameras was used to capture the same view as the ICCD (Raman) camera, and the second was concurrent with the laser, used to align the laser cart and capture tomographic information on the scene.

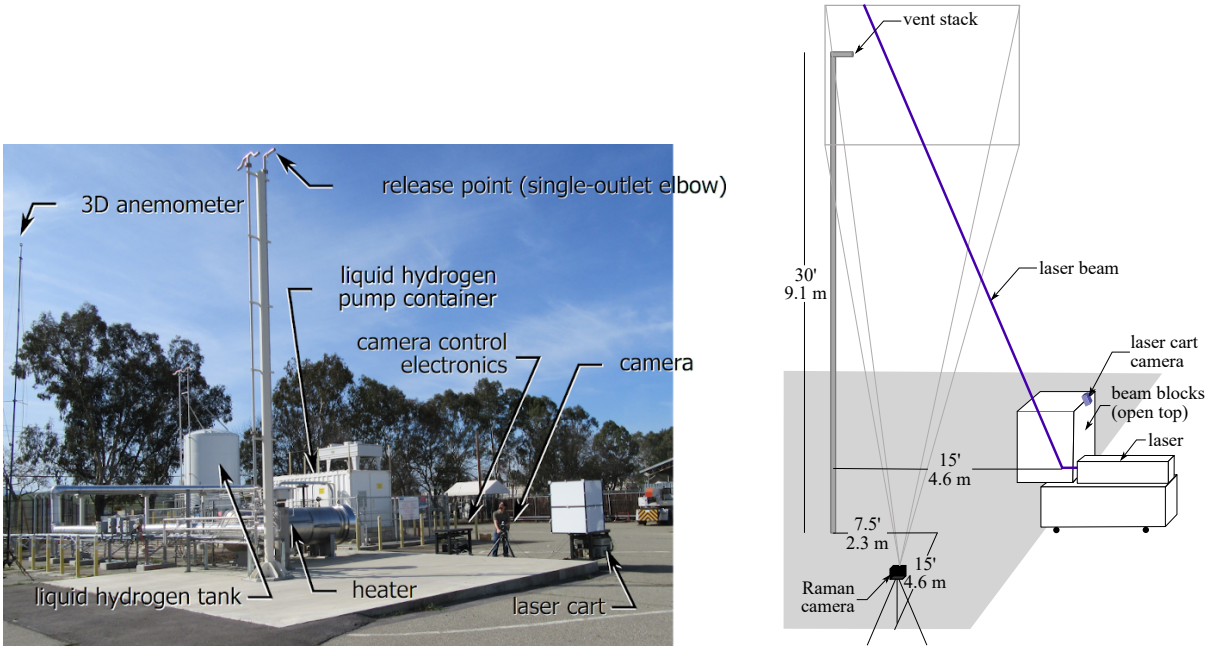

Figure 1. Photo of the experimental equipment (left) and the dimensions and placement of equipment during experimental runs (right).

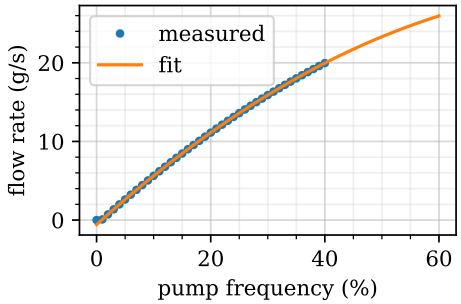

Figure 2. Flow of hydrogen through the pump relative to the frequency.

The laser was directed near the vent stack of a liquid hydrogen tank at Lawrence Livermore National Laboratory, shown in Fig. 1. A more detailed description of the facility is given in [17]. The vent stack is located on a concrete pad away from the liquid hydrogen tank and pump. The stack extends approximately 30 ft (9.1 m) above ground level, and the conventional bullhorns that release hydrogen in two directions were replaced by an elbow and straight 10" (25.4 cm), 2" NPT (2.067" or 52.5 mm ID) section of pipe. Type-E thermocouples inserted into the flow at the bottom and top of the vent stack were used to record hydrogen temperatures. The vent stack is fed from a liquid hydrogen tank and pump with a maximum flowrate of 2 kg/min. Previous experiments were used to relate the pump frequency percentage to flow rate as shown in Fig. 2. A 3D anemometer (Anemeoment TriSonica Mini) also positioned approximately 30 ft (9.1 m) above the ground, offset by about 30 ft (9.1 m) from the vent stack captured wind and weather (i.e. humidity, pressure, temperature) data during experiments.

The equipment was stored in a tent on-site and set up each day when experiments were performed. This required wheeling the laser cart near the pad, aligning it with the vent stack and placing the Raman camera. Because this setup occurred each day of the experiments, there was some change in the alignment of the equipment from day-to-day. The laser cart was placed directly at the edge of the concrete pad, 15 ft (4.6 m) from the vent stack. The Raman camera

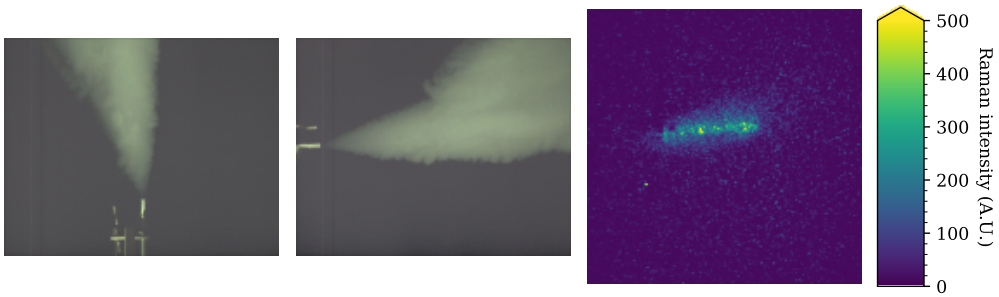

(a) High humidity (RH = 74%), 30% pump speed (15.9 g/s), 95 K H_2 at the vent stack.

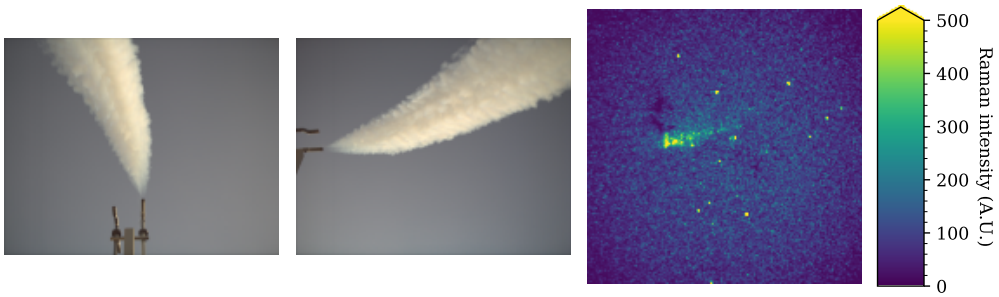

(b) Low humidity (RH = 40%), 30% pump speed (15.9 g/s), 105 K H_2 at the vent stack.

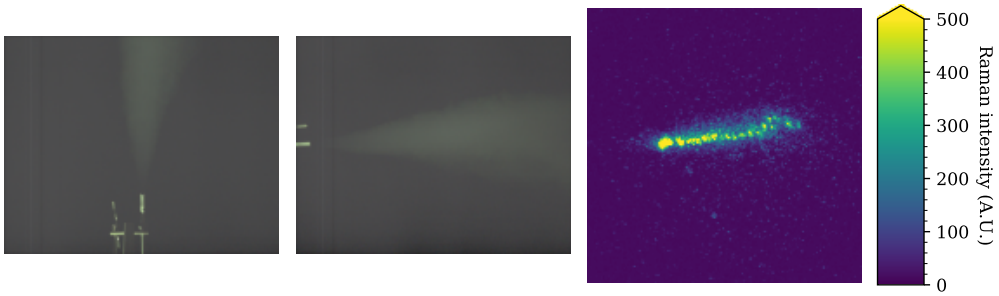

(c) Low humidity (RH = 19%), 40% pump speed (20 g/s), 82 K H_2 at the vent stack..

Figure 3. Integrated visible images (left two frames) and Raman signal (right) for a series of data with a wide range of relative humidity.

was also placed at the edge of the concrete pad halfway between the vent stack and the laser cart. The Raman camera was directed at approximately a 60 degree angle above horizontal so that the vent stack was near the center of the image. With the 25 mm focal length lens, the field of view of the camera at the plane of the vent stack was approximately 17 ft (4.3 m), offering a view of the plume as it extended over the concrete pad. Experiments were performed around and after sunset to reduce the background signal from the sky, which was overwhelming the small Raman signal during initial tests during the day.

3.0 RESULTS AND DISCUSSION

As the liquid hydrogen is pumped through the flow system, heat transfer through the insulation on the lines causes it to vaporize. The hydrogen at the vent stack is cold, but above the saturation temperature at atmospheric pressure (70-110 K) during the release experiments. This is sufficiently cold to condense any moisture that the plume might encounter as it is released. Figure 3 shows the visible plumes from the laser cart (left) and the Raman camera (center) for three separate days of data acquisition. In Fig. 3a, the relative humidity was 74%, while it was much lower (40% and 19%) in Figs. 3b and 3c. The visible images were taken with different illumination (much earlier in the evening for Fig. 3b) and while the wind was fairly

calm during these series of images, there was some variation in the extent to which the plume was blown around. Nonetheless, the visible plumes in Figs. 3a, 3b, and 3c all appear similar in terms of the amount of moisture condensed, the spreading, and trajectory of the visible plume. One might expect additional condensation in the high-humidity case leading to a wider visible plume, but this does not appear to be the case.

The right-hand images in Fig. 3 show the Raman signal as the laser rastered along the plume. Similar to visible images, there is not a large difference in the signals on the three different days. Figure 3b has significantly more background and noise than the Figs. 3a or 3c because it was taken earlier in the evening with more background light. Figure 3c appears to have a bit stronger signal which may be due to the higher pump flowrate during this run. In each of the subfigures, there is scatter near the most intense pixels due to the Raman signal scattering off of the condensed moisture in the plumes. The condensed moisture will attenuate both the excitation light (the laser) and the scattered Raman signal. This attenuation complicates quantification of the Raman signals.

As observed during experiments, even a light breeze ($<$ 2.5 m/s or $<$ 5 mph) can strongly divert the condensed moisture plume. While some evidence in the literature suggests that the hydrogen remains concurrent with the visible moisture plume [10], there is some evidence that flammable concentrations can also be present outside the visible plume [9]. Separation of the hydrogen and the visible plume could occur if the Stokes number for the condensed vapor particles is large enough. In one set of experiments, a breeze blew the visible plume off of the laser line for several laser shots, and then as the laser rastered through the same area, the visible plume remained along the laser line. This series of experiments is shown in Fig. 4. The images are the maximum signal for each pixel over the scan. Figure 4a shows that the laser power remained fairly constant throughout the scan while the laser was projected in-line with the release (y-angle of 0) from near the vent stack (x-angle of -7°), away from the vent stack (x-angle of -2.5°) and back towards the vent stack twice. In the early frames (346-388, covering 4.2 seconds at 10 Hz), the higher wind (see Fig. 4b) blowing in the negative y-direction caused the visible plume to divert from the line along which the laser was rastered, as can be seen in Fig. 4c. In the later frames (389-434, covering 4.5 seconds at 10 Hz), reduced wind (see Fig. 4b) caused the visible plume to be more consistently inline with the laser, as can be seen in Fig. 4d. The extent of the visible plume is roughly traced on the Raman signal contour graph on the right-hand side of Figs. 4c and 4d, and it is clear in the differences between these two plots that in the areas where there is no visible plume, there is also no Raman signal. Some scattered bright marks outside the traced visible area are more likely noise rather than Raman signal. This is strong evidence that the hydrogen is concurrent with the visible plume, regardless of the wind.

In previous works [5, 6] Raman signals were converted to mole fractions and temperatures. Average mole fractions and temperature were compared to the models in HyRAM [18] for validation. The challenge with these outdoor experiments is the unsteadiness of the wind. This prevents the accumulation of a large number of Raman signals for equivalent conditions in a specific location. The signals reported here will be converted to mole fractions, but there will be considerable uncertainty in the measurements due to the low signals. In addition, in the highly turbulent jets/plumes reported here, the instantaneous mole fractions are challenging to use for model validation. The models in HyRAM predict the average concentration, and there is a distribution of concentrations around this average due to the turbulent fluctuations in the plume. Nonetheless, if all of the measured mole fractions fall within the expected distribution at a point in the jet/plume, this will provide strong evidence for a validated model.

During one set of experiments, the high-powered laser caused the vent stack to ignite. While this was not a desired outcome, it was anticipated that this might occur and calculations were

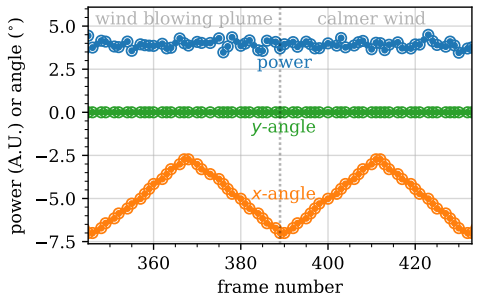

(a) Laser power and angle

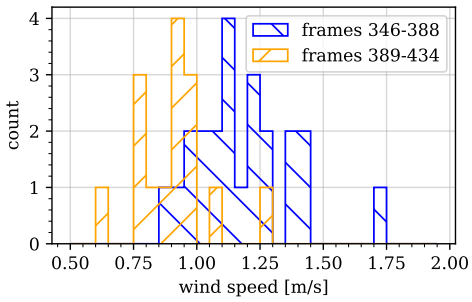

(b) Wind conditions

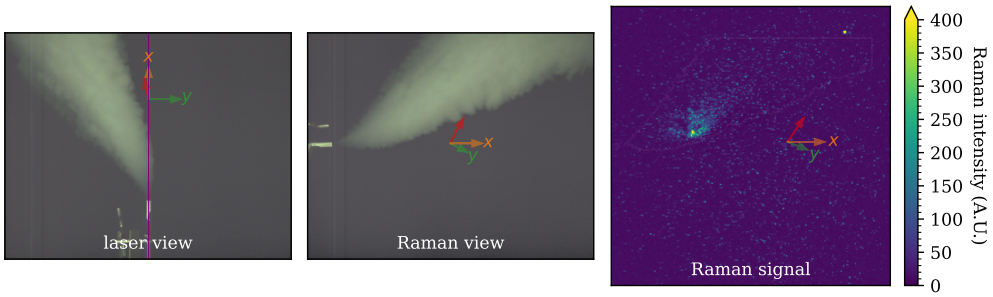

(c) Frames 346-388 (wind blowing plume)

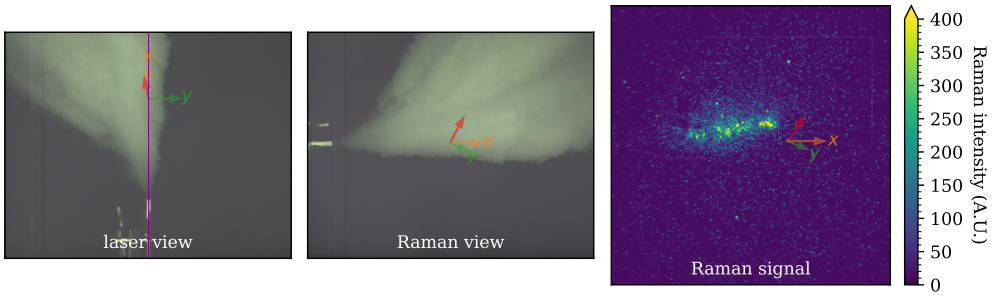

(d) Frames 389-434 (calmer wind)

Figure 4. Experimental results from a single day of testing during windy and calm conditions, with 100 K hydrogen at the vent stack flowing at 15.9 g/s.

made when planning experiments as to the extent of a visible flame and the radiative hazard at ground level from a diffusion flame from the vent stack. The visible images of the ignition phenomena, shown in Fig. 5, provide some data for validation and insights into a hydrogen diffusion flame ignition and burning process. The left-frame of these three images shows that the ignition occurs quite far from the vent stack, towards the bottom of the visible plume. There is initially a large flame, approximately 4 m (13 ft) long and 1.9 m (6.3 ft) wide. After this initial, larger mass of hydrogen has burned out, a more steady diffusion flame develops that is approximately 3 m (9.8 ft) long. The flame has considerable buoyancy, relative to the release and the ignition point is no longer within the burning flame.

4.0 CONCLUSIONS AND FUTURE WORK

In this work, we have presented some initial data from outdoor experiments performed at Lawrence Livermore National Laboratories liquid hydrogen pad. We described a novel laser-based Raman scattering scattering diagnostic that is able to map out the location of hydrogen. The diagnostic rasters a laser, focused near the vent stack 30 ft (9 m) above the ground, at

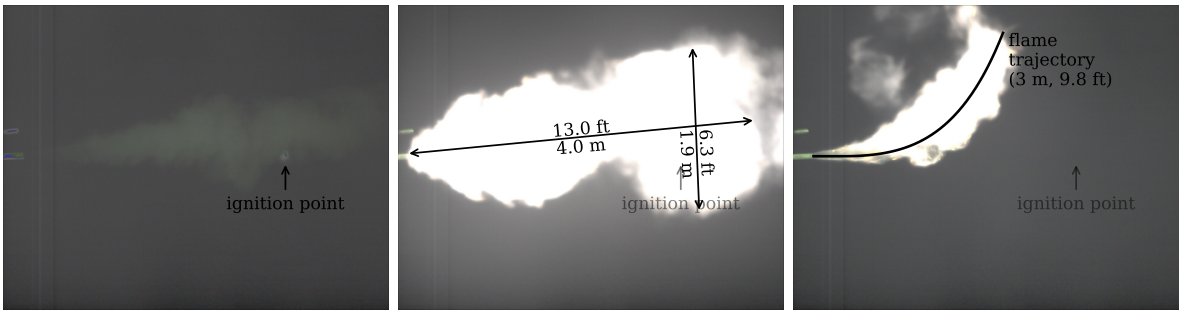

Figure 5. Ignition of the vent stack release, showing an initial ignition kernel (left), the extent of the flame immediately following ignition (center), and the steady flame trajectory and length (3 m long, right).

different angles to probe areas where hydrogen may be present. A gated ICCD camera with a notch filter and time gating to capture only Raman scattered light from hydrogen collects the signal. Visible cameras are used simultaneously to compare where the visible plume and hydrogen are located.

Experiments with different humidity levels (19–74% relative humidity) showed minimal variation in terms of the dispersion of the visible plume. These experiments also demonstrated that the hydrogen is concurrent with the condensed plume, regardless of the humidity level. A light breeze ($<$ 2.5 m/s or $<$ 5 mph) can significantly alter the trajectory of the visible plume. Hydrogen was not observed outside the visible plume, even when the trajectory was altered by the wind. These results indicate that the visible plume is a good indication of the hydrogen location, regardless of the wind or humidity.

In one experiment, the release ignited due to the high-powered laser. Visible images showed that the ignition occurred near the edge of the visible plume, producing an initial fireball that was considerably larger than the steady-state flame. The diffusion flame was quite buoyant.

We plan to perform additional analysis on the experimental data, converting Raman signals to concentration measurements. Due to the low speed nature of the data collection (10 Hz), low signal levels, the turbulent nature of the releases, and the variability in the wind, it will be challenging to use the data for model validation. Nonetheless, the data can demonstrate whether the model is correctly predicting the extent of a flammable concentration, a key parameter for developing safety codes and standards.

5.0 ACKNOWLEDGMENTS

The U.S. Department of Energy's (DOE) office of Energy Efficiency and Renewable Energy's (EERE) Hydrogen and Fuel Cell Technologies Office (HFTO) supports the development of science-based codes and standards through the Safety, Codes and Standards program sub-element. The authors gratefully acknowledge funding from HFTO and the support of subprogram manager Laura Hill for this work. The authors also appreciate Air Liquide and partners for financial support of this work. Sandia National Laboratories is a multi-mission laboratory managed and operated by National Technology and Engineering Solutions of Sandia LLC, a wholly owned subsidiary of Honeywell International Inc. for the U.S. Department of Energy's National Nuclear Security Administration under contract DE-NA0003525. Lawrence Livermore National Laboratory is operated by Lawrence Livermore National Security, LLC, for the U.S. Department of Energy, National Nuclear Security Administration under Contract DE-AC52-07NA27344. This paper describes objective technical results and analysis. Any subjective

views or opinions that might be expressed in the paper do not necessarily represent the views of the U.S. Department of Energy or the United States Government.

REFERENCES

[1] NFPA, NFPA 2: Hydrogen Technologies Code, Tech. rep., NFPA (2020).

[2] J. Xiao, J. Travis, W. Breitung, Hydrogen release from a high pressure gaseous hydrogen reservoir in case of a small leak, International Journal of Hydrogen Energy 36 (3) (2011) 2545–2554.

[3] A. Friedrich, W. Breitung, G. Stern, A. Veser, M. Kuznetsov, G. Fast, B. Oechsler, N. Kotchourko, T. Jordan, J. Travis, J. Xiao, M. Schwall, M. Rottenecker, Ignition and heat radiation of cryogenic hydrogen jets, International Journal of Hydrogen Energy 37 (22) (2012) 17589–17598.

[4] P. P. Panda, E. S. Hecht, Ignition and flame characteristics of cryogenic hydrogen releases, International Journal of Hydrogen Energy 42 (1) (2017) 775–785.

[5] E. S. Hecht, P. P. Panda, Mixing and warming of cryogenic hydrogen releases, International Journal of Hydrogen Energy 44 (17) (2019) 8960–8970.

[6] B. R. Chowdhury, E. S. Hecht, Dispersion of cryogenic hydrogen through high-aspect ratio nozzles, International Journal of Hydrogen Energy 46 (23) (2021) 12311–12319.

[7] E. S. Hecht, B. R. Chowdhury, Characteristic of cryogenic hydrogen flames from high-aspect ratio nozzles, International Journal of Hydrogen Energy 46 (23) (2021) 12320–12328.

[8] A. Friedrich, A. Vesser, T. Jordan, PRESLHY experiment series E3.1 (cryogenic hydrogen blowdown/discharge) results.
URL http://dx.doi.org/10.5445/IR/1000096833

[9] Arthur D. Little, Inc., Final report on an investigation of hazards associated with the storage and handling of liquid hydrogen, Tech. rep. (1960).

[10] M. G. Zabetakis, A. L. Furno, G. H. Martindill, Explosion Hazards of Liquid Hydrogen, in: Adv. Cryog. Eng., Vol. 8324, Springer US, Boston, MA, 1961, pp. 185–194.

[11] R. Witcofski, J. Chirivella, Experimental and analytical analyses of the mechanisms governing the dispersion of flammable clouds formed by liquid hydrogen spills, Int. J. Hydrogen Energy 9 (5) (1984) 425–435.

[12] U. Schmidtchen, L. Marinescu-Pasoi, K. Verfondern, V. Nickel, B. Sturm, B. Dienhart, Simulation of accidental spills of cryogenic hydrogen in a residential area, Cryogenics (Guildf). 34 (1994) 401–404.

[13] M. Royle, D. Willoughby, Releases of unignited liquid hydrogen, Tech. Rep. RR986, Health and Safety Executive (2014).

[14] J. Hall, Ignited releases of liquid hydrogen, Tech. Rep. RR987, Health and Safety Executive (2014).

[15] DNV GL Oil and Gas, Liquid hydrogen safety data report: Outdoor leakage studies, Tech. Rep. 853182, Forsvarets forskningsinstitutt (FFI) NorwegianDefence Research Establishment, available at https://www.vegvesen.no/_attachment/2997130/binary/1373429 (2020).

[16] K. Lyons, S. Coldrick, G. Atkinson, Summary of experiment series e3.5(rainout) results, Tech. rep., available at https://hysafe.info/wp-content/uploads/sites/3/2020/08/PRESLHY_D3.6_Summary_of_Rainout_Experiments_V1.20.pdf (2020).

[17] G. Petitpas, S. M. Aceves, Liquid hydrogen pump performance and durability testing through repeated cryogenic vessel filling to 700 bar, International Journal of Hydrogen Energy 43 (39) (2018) 18403–18420.

[18] B. D. Ehrhart, E. S. Hecht, Hydrogen risk assessment models (HyRAM) version 3.1 technical reference manual, Tech. Rep. SAND2021-5812, Sandia National Laboratories (2021).